Available online at www.sciencedirect.com
ScienceDirect
Polymer 48 (2007) 1500–1509
polymer
www.elsevier.com/locate/polymer

Hyperbranched polyol/carbon nanofiber composites

Susan M. Rhodes*, Bernadette Higgins, Yijin Xu, William J. Brittain

Department of Polymer Science, The University of Akron, Akron, OH 44325, USA

Received 4 October 2006; received in revised form 17 January 2007; accepted 19 January 2007
Available online 25 January 2007

Abstract

Carbon nanofiber (CNF) and carbon nanotube (CNT) composites have enhanced mechanical and electrical properties that make these composites desirable for antistatic and electronic dissipation technology. These applications require a homogenous dispersion of CNFs within a polymer matrix. To improve the compatibility/dispersability of CNFs within a polymer matrix, a hyperbranched polyol CNF composite was synthesized by the chemical modification of oxidized CNFs with glycidol and boron trifluoride diethyl etherate. The resulting polyol CNFs were characterized by TGA, FTIR, TEM/SEM and XPS. The hydroxyl groups were reacted with heptafluorobutyryl chloride to determine the amount of oxidized groups in the sample. The resulting composite was characterized by FTIR and elemental analysis. The amount of hydroxyl groups increased by 550% for the polyol CNFs as compared to the oxidized CNFs and an improvement in dispersion ability was observed.

Keywords: Carbon nanofibers; Surface-induced polymerization; Dispersion

1. Introduction

Carbon nanofiber (CNF)/polymer composites have been investigated for enhanced mechanical, thermal and electrical properties of polymers [1,2]. The main focus of this research is to provide improved electrical properties of polymers through the network formation of CNFs at low weight percent (percolation threshold) in polymer composites. Electrically conductive or semiconductive composites could be used for electrostatic dissipation (ESD) and electromagnetic/radio frequency interference (EMI/RFI) protection, as well as electronic biological sensing [3–15].

To obtain percolation in CNF composites, the CNFs must be homogenously dispersed within the polymer matrix [1]. The use of mechanical and/or chemical forces is required to break-up CNF aggregates prior to composite formation [1,16]. High shear methods have been utilized to effectively disperse CNFs; however, this method often results in a breaking/shortening of the CNFs. The decreased aspect ratio leads to ineffective property improvement of the CNF composite [17]. One alternative to this high shear methodology is chemical modification of CNFs to improve the interaction between CNFs and the polymer matrix [16,18]. This technique decreases the aggregation of the CNFs, however, the extent of fiber shortening is much less than high shear methods. Chemically assisted dispersion in polar media was theorized possible if a hyperbranched polyol could be polymerized from the surface of the CNFs.

Glycidol, a hydrophilic trifunctional (AB_2) monomer, was used to produce a hyperbranched polymer on CNFs [19]. This monomer can be polymerized *via* a cationic or anionic mechanism depending upon the initiator used. One common initiator for the cationic synthesis is boron trifluoride diethyl etherate (BF_3OEt_2) [20,21] and was used in this research. BF_3OEt_2 provided a number-average molecular weight of 500–3000 g/mol, while lower reaction temperature provided higher molecular weight. NMR studies showed that monomer addition is a combination of activated monomer and activated chain end mechanisms. Activated monomer addition produced primary and/or secondary alcohols, while activated chain end addition produced only primary alcohols [21].

Royappa et al. cationically synthesized polyglycidol at room temperature [22]. Xu et al. performed surface-induced polymerization of a highly strained hydrophilic monomer,

---

* Corresponding author. Tel.: +1 330 972 5388; fax: +1 330 972 5461.
E-mail address: smr40@uakron.edu (S.M. Rhodes).

0032-3861/$ - see front matter © 2007 Elsevier Ltd. All rights reserved.
doi:10.1016/j.polymer.2007.01.038

3-ethyl-3-(hydroxymethyl) oxetane, with oxidized multi-walled carbon nanotubes (MWNT) with BF_3OEt_2 [23]. Hong et al. prepared hyperbranched polymers on MWNT using ATRP [24].

An aspect of hyperbranched/CNF research that has not been explored yet is a one-step surface-induced synthesis of a hyperbranched polymer on CNFs. The increased amount of hydroxyl groups on the surface of the CNFs will aid in dispersability of hydrophilic solvents and polymers (*e.g.* PVOH, epoxy). To compatibilize CNFs with other polymers, such as polystyrene and poly(methyl methacrylate), radical polymerizations could be used to surface modify CNFs.

The surface-induced polymerization of oxidized carbon nanofibers by glycidol is reported. The resulting polyol-modified CNFs were characterized by SEM/TEM, FTIR, and TGA. The hydroxyl groups were reacted with heptafluorobutyryl chloride to determine the amount of oxidized groups in the sample. The resulting composite was characterized by FTIR, TGA, and elemental analysis. Solubility, aggregation, and dispersion studies were performed to determine the compatibility of the oxidized CNFs and modified CNFs with other materials.

2. Experimental

2.1. Materials

All materials were used as received unless otherwise noted. Pyrograf III (PR-24-PS-LD-OX) oxidized carbon nanofibers were provided by Applied Sciences, Inc. These fibers have a diameter of 60–150 nm, a fiber length of 50–100 μm, a dispersive surface energy of 75–95 mJ/m^2 and a N_2 surface area of 40–50 m^2/g (data provided by Applied Sciences, Inc.). Glycidol (96%) was purchased from Aldrich and dried over 4Å molecular sieves for three days; the purity was confirmed by NMR analysis. Anhydrous methylene chloride, anhydrous acetonitrile, heptafluorobutyryl chloride (98%), boron trifluoride diethyl etherate (filtered, redistilled), potassium bromide (IR grade), pyridine (ACS grade, purified and redistilled) and anhydrous *o*-dichlorobenzene were purchased from Aldrich. Methanol (ACS grade), ethylene glycol, and acetone (HPLC grade) were purchased from Fisher Scientific. Carbon coated copper grids were purchased from SPI supplies. PTFE filter paper (0.2 μm pore size) was purchased from Fisher Scientific. Probe sonication was performed with a GE model 130 probe sonicator at 60% amplitude.

2.2. Surface-induced polymerization of CNF with glycidol (CNF-polyol)

Oxidized CNF (CNF-OX) (0.5 g) was charged into a 100 mL Schlenk flask and dried under vacuum at 130 °C for 3 h. The flask was cooled to RT and closed to vacuum. Anhydrous methylene chloride and BF_3OEt_2 were added, 35–40 mL and 200 μL, respectively. The solution was degassed and placed under positive nitrogen pressure. The flask was then cooled to −20 °C. Glycidol monomer, 7 mL, was then added while stirring over 30 min *via* a syringe pump. The reaction was kept cold until a phase separation was observed. After 24 h, the solvent was decanted and the solid material left was dispersed in 250 mL MeOH. The solution was covered and stirred for 24 h (to completely remove free polymer). The modified CNFs were collected by suction filtration, washed with 5 × 100 mL MeOH, and then dried under vacuum at RT.

2.3. Free glycidol polymerization

Free glycidol polymer was obtained using the same procedure noted above, however, without the use of CNF-OX. Instead of filtration with MeOH, approximately 25% of MeOH was allowed to evaporate and the free polymer was precipitated from acetone (150 mL) and filtered through a PTFE filter. The polymer was then dried under vacuum at RT for 24 h. All of the solvent could not be removed due to extensive hydrogen bonding with the polymer.

2.4. Physical mixing of CNF-OX with free polyol

CNF-OX (0.1 g) was charged into a beaker with 50 mL MeOH. Free polymer of 2.5 wt% (2.5 mg) was added to the stirring MeOH mixture. The solution was sonicated for 5 min and then allowed to stir for 24 h. MeOH was removed *via* evaporation and the resulting product was dried under vacuum for 24 h.

2.5. Acid–base titration of CNF-OX

Determination of acidic sites of purified SWNT by acid–base titration was discussed by Hu et al [25]. The forward titration method with $NaHCO_3$ was used to determine the number of carboxylic acid sites, while the total number of acidic sites (carboxyl and hydroxyl) were determined using NaOH in place of $NaHCO_3$.

2.6. Esterification of CNF-OX and CNF-polyol with an acid chloride

This procedure was based on the previous literature reactions with modifications for oxidized CNFs [26]. A 50 mL Schlenk flask was charged with 0.1 g CNF-OX (or CNF-polyol). The sample was dried for 3 h at 130 °C under high vacuum. After cooling to room temperature (RT) and backfilling with N_2(g), 30 mL anhydrous acetonitrile and 0.68 mL pyridine were charged into the flask. The contents were then degassed using 3 freeze/pump/thaw cycles. Using a syringe, 1 mL heptafluorobutyryl chloride was charged into the flask manually over 15 min. The contents were then mixed for 24 h at 30 °C. The flask was opened to air and MeOH was added drop wise to react with any excess acid chloride, until no further HCl gas was generated upon its addition. The contents were filtered through a 0.2 μm polycarbonate membrane and washed with 3 × 50 mL MeOH followed by 50 mL H_2O. The modified fibers were dried at RT under high vacuum for 3 h.

2.7. Aggregation study of CNF-OX and CNF-polyol

CNF-OX and CNF-polyol were weighed into vials with either water or *o*-dichlorobenzene at a weight ratio of 10,000/1 of solvent/CNF. The solutions were probe sonicated for 1 min each and deposited immediately onto carbon coated 400-mesh Cu TEM grids.

2.8. Dispersion study of CNF-OX and CNF-polyol

To determine the dispersion ability of CNF-OX and CNF-polyol, the fibers were placed into vials with water at various concentrations, followed by probe sonication. The samples were observed over a six-week period and any settling of the fibers to the bottom of the vials was recorded.

2.9. Instrumental methods of characterization

TGA measurements were made using a Hi-Res TGA 2950 thermogravimetric analyzer (TA Instruments) at a heating rate of 10 °C/min in air. FTIR measurements were made using a Nicolet 730 spectrophotometer with KBr pellet or salt plate. TEM micrographs were made using a FEI Technai 12 transmission electron microscope, with samples dispersed in water or organic solvent at a concentration of 10,000/1 w/w solvent/CNF. SEM micrographs were made using a Jeol JSM-5310 scanning electron microscope. Samples were sputter coated with a Au/Pd alloy (40:60). GPC results were obtained with a Waters 410 differential refractometer with Waters Styragel columns (HR4 and HR2) in DMF at 50 °C and a flow rate of 0.7 mL/min using a concentration of 10–15 mg/4 mL and polystyrene standards for calibration. NMR analysis was performed using a Mercury 300 MHz NMR with Mestre C software. Samples were dissolved in DMSO-d_6. Elemental analysis was performed by Galbraith Laboratories. XPS measurements were performed using Perkin–Elmer PHI-5600 system at Case Western Reserve University using a 45° take-off angle. Peak deconvolution of XPS multiplex scans in the C1s and O1s regions, 280–295 eV and 526–540 eV, respectively, was performed using a non-linear least squares curve fitting program with a Gaussian–Lorentzian mix function.

3. Results

3.1. Analysis of free polyglycidol by ^{1}H, ^{13}C NMR and GPC

Free polymer showed a broadening of the peaks in ^{1}H NMR compared with the monomer that was dried over molecular sieves (Fig. 1(a) and (b)). ^{13}C NMR shows that there was polymer formed with no residual monomer due to the absence of the monomer peaks at 63, 52, and 43 ppm (Fig. 2(a)).

GPC-DMF results showed that there were three different molecular weights in the free glycidol polymer. The first peak was bimodal with a M_n of 1,131,000 g/mol, M_w of 2,184,000 g/mol, and a PDI of 1.93. The second peak had a M_n of 5500 g/mol, M_w of 9000 g/mol, and a PDI of 1.63. The third peak which was attributed to tetramers had M_n of 290 g/mol, M_w of 320 g/mol, and a PDI of 1.09. The area of the peaks were calculated *via* Viskotek's software and weighing the peaks that were printed on paper and provided consistent results. The contribution of high molecular weight material is 24%, while 48% is due to 5500 g/mol material and 28% is due tetramers (27%, 47% and 26%, respectively, using the paper method).

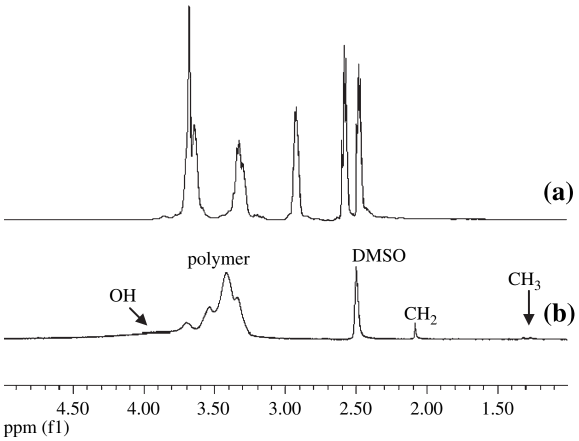

Fig. 1. ^{1}H NMR of (a) glycidol monomer over molecular sieves (CDCl$_3$) and (b) glycidol free polymer (DMSO) (b).

3.2. SEM/TEM analysis

SEM and TEM micrographs show that Pyrograf III oxidized CNFs have conical graphitic planes that intersect a hollow center, in which the planes are oriented almost parallel to

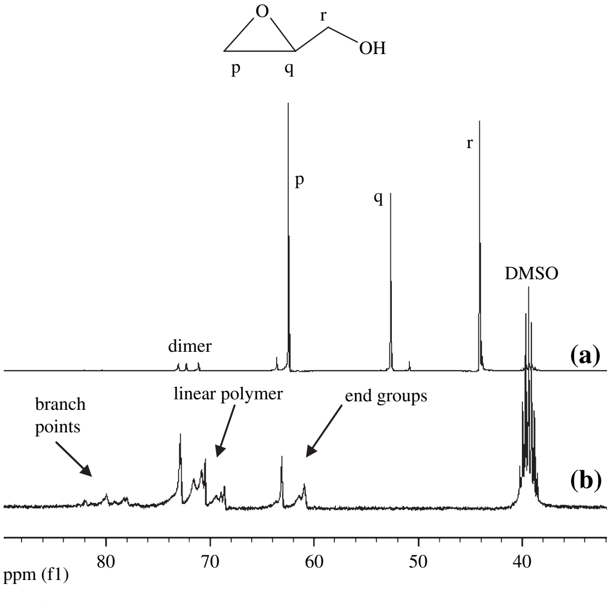

Fig. 2. ^{13}C NMR carbon assignments for the monomer and polymeric groups of (a) glycidol monomer dried over molecular sieves and (b) free polyol in d_6-DMSO.

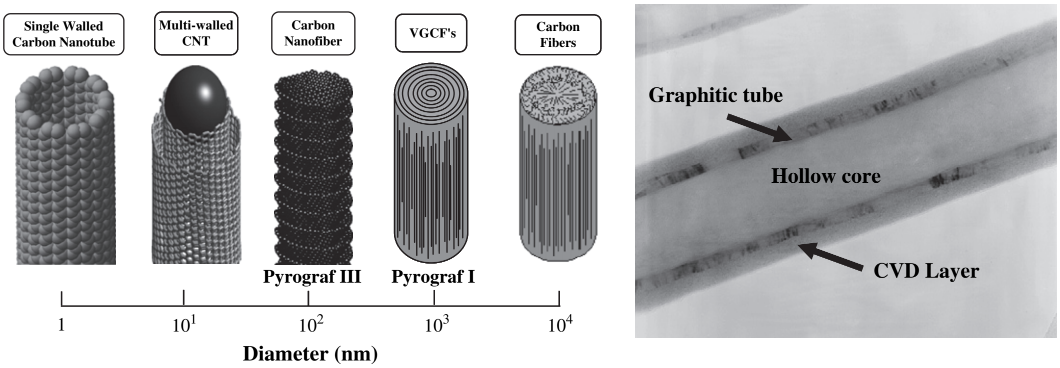

Fig. 3. (1) Schematic of carbon fibers and tubes of various sizes and (2) transmission electron micrograph of carbon nanofibers (pictures provided by Applied Sciences, Inc.).

the fiber axis (a highly oblique angle). There is scattered evidence of bamboo-like structure. These fibers do not contain a chemical vapor deposition layer (Fig. 3(a) and (b)).

TEM micrographs of the CNF-polyol showed polymer on the surface of the fibers by visual inspection (Fig. 4). There was no way to determine visually if the polyol was covalently bonded to the CNFs, but the polymer was strongly adhered to the CNFs (Fig. 4(b)), and adhered to itself in polymer aggregates (Fig. 4(c)). On average, it was found that the CNF-polyol had an increased diameter of about 50 nm as compared to the CNF-OX. This increase in diameter is due to the polymer attached to the fibers. Several TEM images were used to determine the fiber diameters for both samples. It was assumed that the average diameter measured from several images was representative of the whole sample. CNF-OX and CNF-polyol fibers have a diameter range of 60–150 nm and 107–204 nm, respectively.

3.3. FTIR spectroscopic analysis of surface functionality

Analysis of the FTIR spectrum for CNF-OX shows a broad OH peak at 3400 cm^{-1} with a shoulder toward the lower frequency indicating OH stretch from an acid group. A peak at 1620 cm^{-1} is due to conjugated aromatic C=C, however, there may also be a contribution of broadness of this peak due to conjugated C=O from quinoid structure on the CNFs (as indicated by XPS). Another broad peak at 1070 cm^{-1} is due to the C–O stretch of ether, ester, alcohol and anhydride.

Fig. 5 shows the FTIR spectra for the CNF-OX, CNF-polyol, and free polyol. Some spectral changes in the CNF-polyol spectrum (Fig. 5(a)) compared to CNF-OX (Fig. 5(b)) include the appearance of aliphatic $\mathrm{CH_2}$ at 2900 cm^{-1}, a broad C–O stretch at 1300–1500 cm^{-1}, and increased intensity of the C–O ether stretch at 1100 cm^{-1}. The characteristic stretches from the polyol can be seen in the free polymer (Fig. 5(c)).

3.4. TGA analysis of thermal stability and amount of attached polyglycidol

TGA analysis indicates the CNF-OX has a degradation temperature of 580 °C, with a smaller weight loss peak at 380 °C. Fig. 6 shows the TGA scans of CNF-OX, polyol CNF and the free polyol. Fig. 6(a) shows derivative weight percent for these materials showing the rate at which the material is decomposing and the peak decomposition temperature. Fig. 6(b) shows the weight percent loss curve with respect to temperature. In Fig. 6(b), the free polymer had a weight loss of 10% before 200 °C due to solvent in the polymer from hydrogen bonding. Extensive use of vacuum could not remove the solvent (one week at 50 °C). Assuming all free polymers in the CNF-polyol were removed, the TGA indicates that 2.5 wt% polyol is attached to the CNFs at 275–300 °C.

Thermal stability of the covalent *vs.* physical attachment of glycidol to the CNFs was investigated. One sample used CNF-OX that had been stirred with 2.5 wt% free polymer

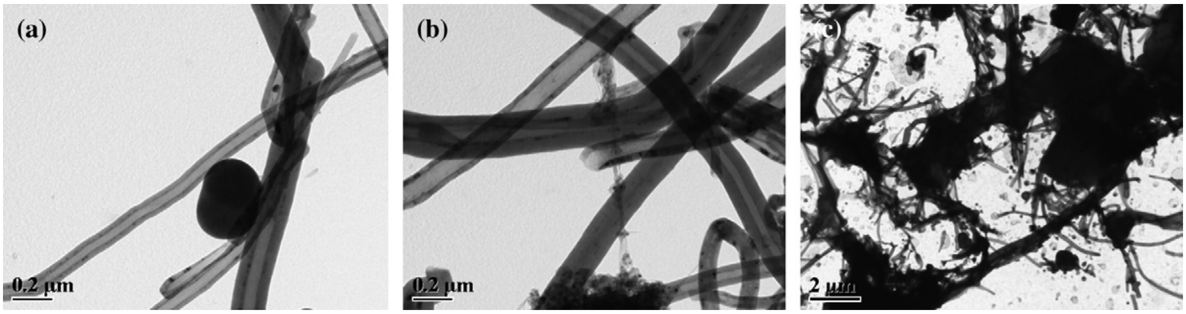

Fig. 4. TEM images of CNF-polyol composites: (a) oxidized CNF, (b) CNF-polyol, and (c) CNF-polyol with polymer aggregate.

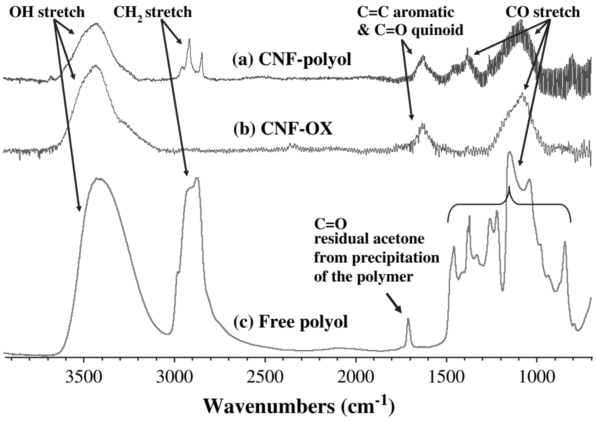

Fig. 5. FTIR of (middle) oxidized CNF, (top) CNF-polyol, and (bottom) free polyol.

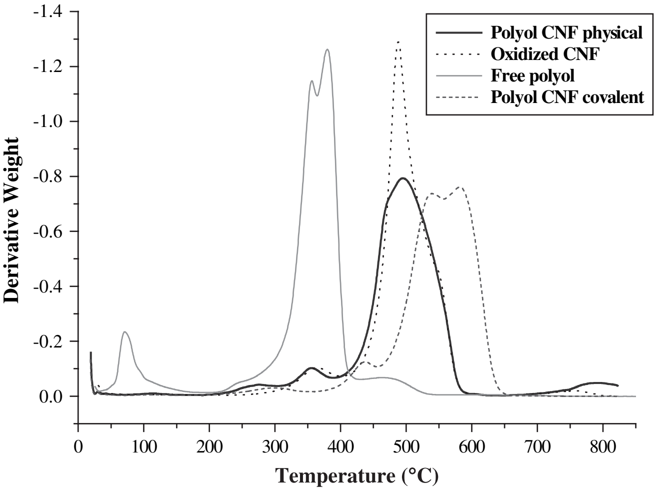

Fig. 7. CNFs physically mixed with glycidol compared with the free polymer, CNF start, and CNF covalently attached.

and another sample used CNF-polyol. The purpose for these experiments was to determine if the thermal stability increase was due to a covalent CNF/polymer bond or if a physical interaction would produce similar increased thermal stability. Fig. 7 shows the resulting derivative TGA plot, including CNF-OX, CNF-polyol (covalent), CNF-polyol (physical), and free polyol polymer. The physically mixed CNFs show no increase in thermal stability or change in shape of the main decomposition peak at 500 °C. There was a small peak for the polymer decomposition at 275 °C for the physical CNF-polyol, which was at the same temperature as the polyol in the covalent CNF-polyol. The amorphous carbon peak in the physically mixed CNFs was at the same temperature (350 °C) as the CNF-OX amorphous carbon peak.

3.5. Surface group determination by XPS

XPS revealed 86.2 at% carbon and 13.8 at% oxygen, normalized, for CNF-OX. Deconvolution of the O1s peak indicates two main types of oxygen groups, COOH/OH and quinoid in ∼40:60 ratio [27] (Fig. 8). These data were used to determine how many reactive functional groups were present in the CNF-OX, as only the carboxyl and hydroxyl groups could be utilized. XPS was not run on CNF-polyol because complete solvent removal was not achieved (as mentioned in Section 3.4) and oxygen content would be influenced by absorbed moisture of the sample due to its hydrophilic nature which would vary with fiber aggregation.

3.6. Reactive oxygen functionality determination by acid–base titration

Titration with $NaHCO_3$ and NaOH revealed the mole percentage of carboxyl groups in the oxidized CNFs to be 3.5%, while the total acid was 5.0%. These results are consistent with XPS analysis.

3.7. Esterification results

The modified CNFs were analyzed by TGA which showed two weight loss peaks, 648 °C (anhydride product) and 728 °C (ester product). Fig. 9(a) shows the FTIR spectra of CNF-OX and the fluorinated CNF-OX (CNF-OX-F). After esterification, the C=C/C=O (1600–1730 cm^{-1}) peak became slightly

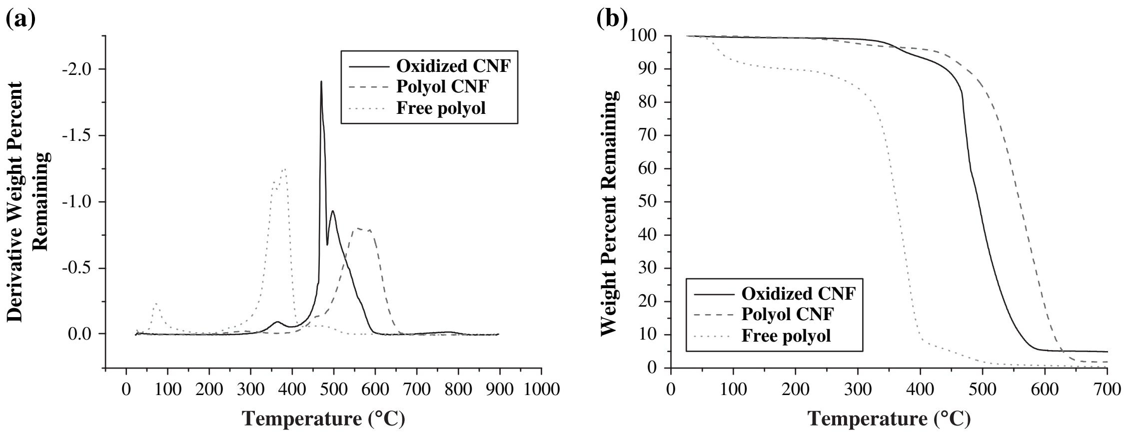

Fig. 6. TGA of CNF/glycidol samples (a) derivative weight curves and (b) weight percent loss curves.

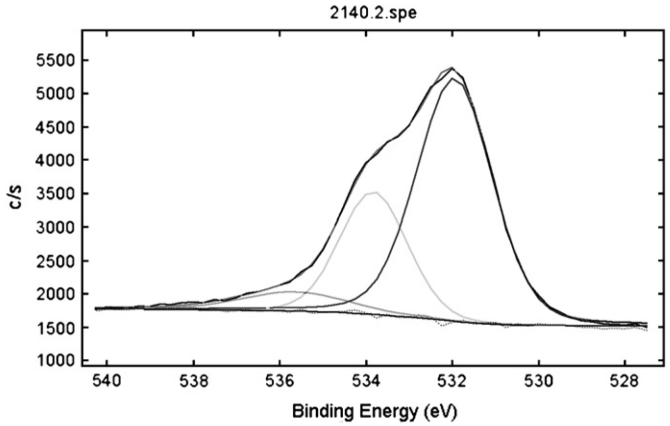

Fig. 8. XPS multiplex scan of O1s region for oxidized carbon nanofibers and its corresponding deconvolution.

larger and broadened. New peaks are visible at 1500 cm^{-1} (fused aromatic), 1400 cm^{-1} (aromatic C—C), 1300 cm^{-1} (CF_3), 1100 cm^{-1} (ether and CF_2), 900 cm^{-1} and 800 cm^{-1} (fused aromatic).

Fig. 9(b) shows the FTIR spectra of CNF-OX, CNF-polyol, and fluorinated polyol CNF (polyol CNF-F). Several new peaks and changes in peak shapes were observed. These peaks include C=C/C=O from the CNFs (1600–1730 cm^{-1}), aromatic C—C (1400 cm^{-1}), CF_3 (1300 cm^{-1}), CF_2 and C—O—C (1100 cm^{-1}) and fused aromatic (800 cm^{-1}).

Elemental analysis confirmed the presence of fluorine attached to the CNFs as well as unreacted oxygen (quinoid). Results are shown in Table 1. The esterified CNF-OX and CNF-polyol samples gave 6900 ppm and 37,400 ppm F, respectively.

3.8. Aggregation study in two different solvents with CNF-OX and CNF-polyol

To further investigate the theory of a polymer coating on CNF-polyol, aggregation of CNF-OX and CNF-polyol were studied using two solvents, water and *o*-dichlorobenzene (*o*-DCB). CNF-OX and CNF-polyol were weighed into vials with solvent using a weight ratio of 10,000/1 of solvent/CNF. The solutions were sonicated for 1 min each and deposited immediately onto TEM grids and dried under vacuum. Results are shown in Fig. 10(a)–(d). Fig. 10(a) shows that the CNF-polyol had aggregated significantly in *o*-DCB, but not in water (Fig. 10(b)). The dispersion of CNF-polyol in water (Fig. 10(b)) improved significantly, with CNFs having only 5–10 nanofibers per aggregate, as determined by counting the number of fibers in several TEM images.

Table 1
Elemental analysis results of the oxidized CNFs and CNF-glycidol functionalized with a fluorinated acid chloride

Type of CNF	ppm F	Moles OH	Number of OH groups	Weight percent OH
CNF-OX-F	6900	5.1×10^{-5}	3.1×10^{19}	0.1
Polyol CNF-F	37,400	2.8×10^{-4}	1.7×10^{20}	0.5

In Fig. 10(c) and (d), the opposite trend was observed. The CNF-OX is more stable in *o*-DCB than in water resulting in single CNF or small aggregates (Fig. 10(c)) in *o*-DCB. The aggregation of CNF-OX in water was significantly more than in *o*-DCB, but less aggregated compared with CNF-polyol in *o*-DCB. The lack of significant aggregation was due to the CNFs having oxidized groups which partially stabilize the CNFs in water.

3.9. Dispersion study of CNF-OX and CNF-polyol in H_2O

CNF-polyol dispersion ability and macroscopic stability in solution were determined by dispersing both CNF-polyol and CNF-OX in water for four weeks. Fig. 11(a) shows the CNF-polyol that had been sitting for four weeks. The concentrations vary from left to right at 0.1–5 wt% with polyol content of about 18 wt%. Fibers remained suspended for the duration of the study. Fig. 11(b) shows the CNF-OX after only two

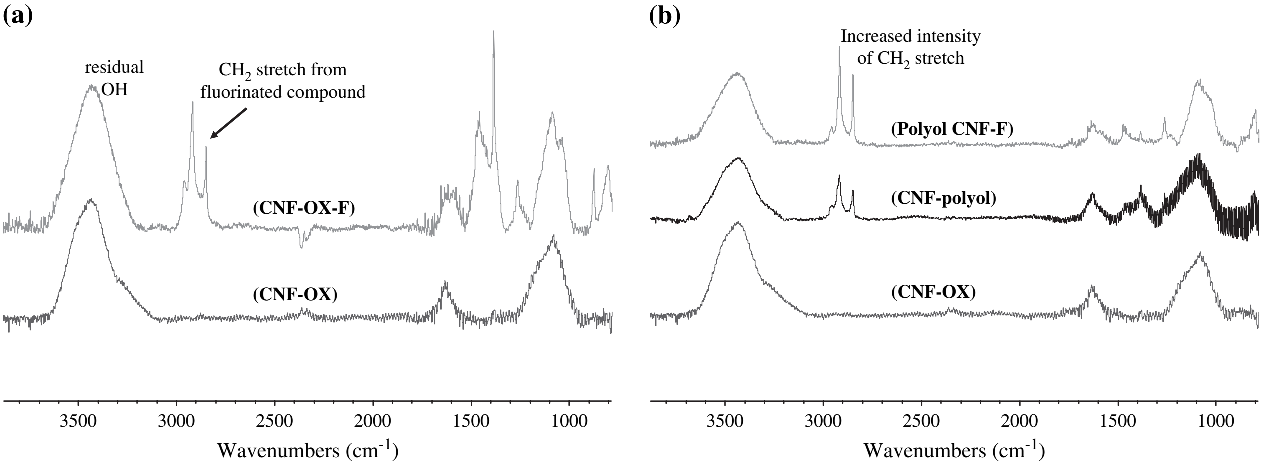

Fig. 9. FTIR of (a) fluorinated oxidized CNF (top) and oxidized CNF (bottom), and (b) oxidized CNF (bottom), CNF-polyol (middle) and fluorinated CNF-polyol (top).

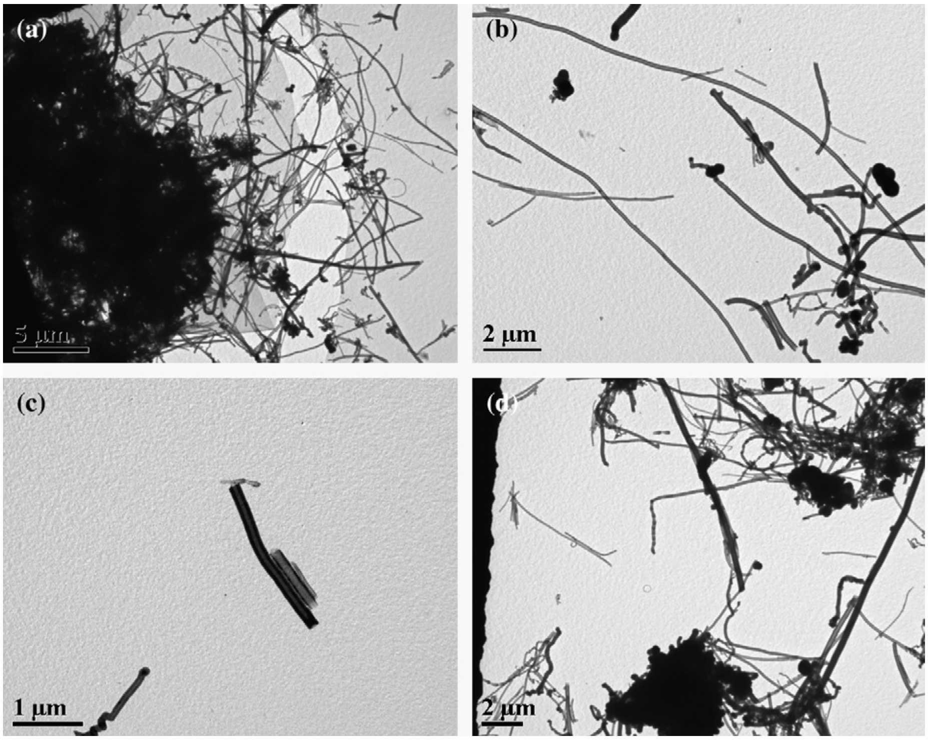

Fig. 10. Polyol CNFs deposited from (a) *o*-DCB and (b) water, and oxidized CNFs deposited from (c) *o*-DCB and (d) water at a concentration of 10,000/1 (solvent/CNF w/w).

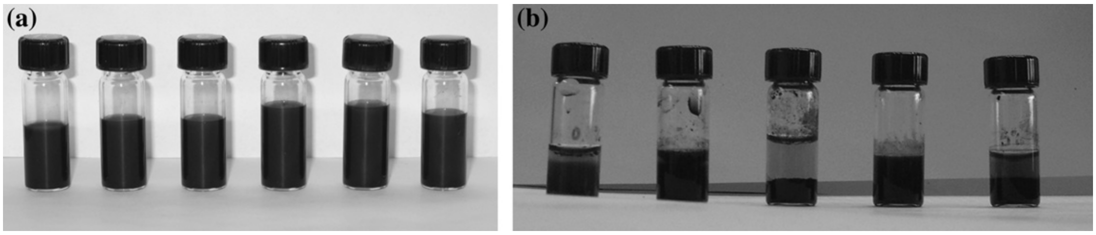

Fig. 11. Pictures of the dispersion of the oxidized polyol CNFs after four weeks and the oxidized CNFs with no functionality after two weeks.

weeks (at the same concentrations) and already the fibers have settled to the bottom of the vials.

4. Discussion

Glycidol monomer is highly reactive due to the strained epoxide ring. Synthesis of glycidol functionalized CNFs was performed according to Scheme 1. The alcohol and carboxylic acid groups on the surface of CNF-OX were the only groups capable of reacting with glycidol and the BF_3OEt_2 initiator, resulting in ether and ester linkages of polyol to CNFs. In the presence of BF_3OEt_2 initiator, this reaction is exothermic and requires a cold temperature (−20 °C) during polymerization. A phase separation was observed after 5 min to 5 h; after which the reaction was allowed to proceed for 24 h at 25 °C. The reason for the variable precipitation time for the CNFs

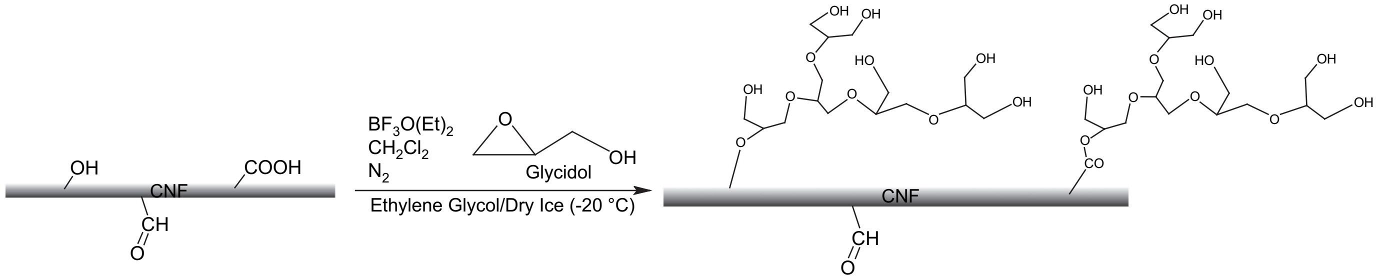

Scheme 1. Hyperbranched polyol synthesis of CNFs.

may be temperature changes or heterogeneity of the CNFs (specifically, heterogeneity of oxidized groups and aggregation of CNFs). Based on the GPC trace, it can be concluded that there is little control over this reaction due to the polymer chains having both large and small molecular weight peaks ($M_n = 1{,}131{,}000$ and $M_n = 290$ g/mol).

The grafting procedure reported here is simpler than the typical three steps reported in the literature [23,24]. In the literature, the carboxylic acid groups are generated *via* nitric/sulfuric acid treatment, converted to acid chlorides, then to alcohol groups prior to reaction with a strained oxirane ring [23,24]. Our reaction was using the oxidized CNFs from Applied Sciences, Inc.

The TEM images showed that if good dispersion was not achieved prior to polymerization, the polymer appeared to polymerize the aggregated CNF-OX (Fig. 4(c)). The polymer layer is present as a coating that surrounds several fibers. The polymerized aggregated CNF-polyol was more difficult to separate than the CNF-OX because hydrogen and covalent bonds hold the aggregates together, instead of only weak interactions (van der Waals and $\pi-\pi$ attractions). Only smaller aggregates could be obtained after sonication.

The degradation temperature, as measured by TGA, of CNF-OX is much lower than other types of CNFs, such as heat treated and pyrrolytically stripped fibers ($T_d > 600$ °C) (Fig. 12(a)–(c)). It has been observed in the literature that peaks before the final decomposition of CNFs (∼600 °C) are due to amorphous carbon (300–400 °C) [16]. In Fig. 6(a), the amorphous carbon appears at about 350 °C. For the CNF-polyol, the amorphous carbon peak has moved from 350 °C (CNF-OX) to a shoulder on the main decomposition peak at higher temperature, 400 °C. This indicates that the outer rings of the CNFs became more thermally stable and made them less susceptible to oxidation and decomposition, resulting in increased thermal stability of the CNFs.

The CNF-OX and CNF-polyol were reacted with heptafluorobutyryl chloride (Scheme 2) to determine the amount of reactive oxygen functional groups on the fibers. This particular fluorinated compound was used because of increased signal (seven fluorine atoms for every hydroxyl group that reacted). It was assumed that by using the heptafluorobutyryl chloride in 100 fold excess, all reactive groups on the surface of the CNF-OX and CNF-polyol would react. The lack of polarity of acetonitrile resulted in some aggregation of the CNF-polyol and CNF-OX; however, the fibers remained suspended for the full reaction time after sonication. The resulting esterified CNFs appeared similar to CNF-OX and CNF-polyol and were no longer dispersible in methanol.

After the esterification reaction, there were significant amounts of acid chloride remaining in the reaction solution

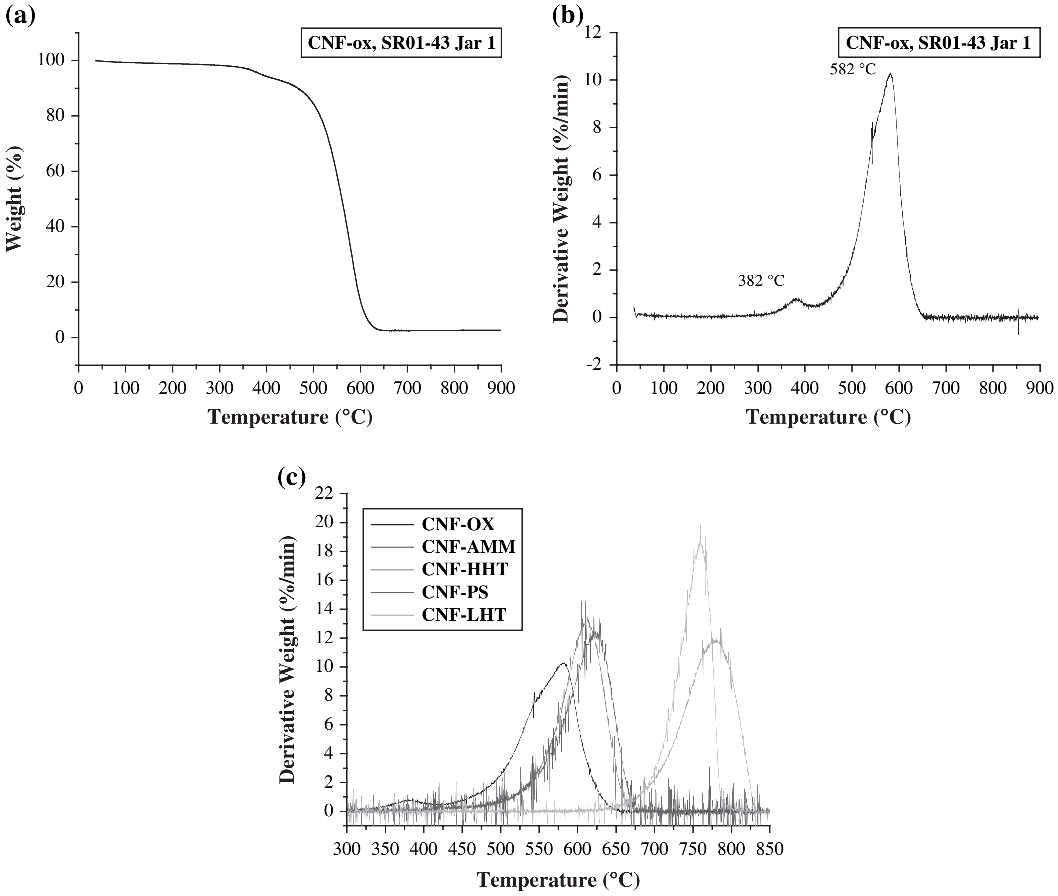

Fig. 12. TGA plot of (1) weight percent, (2) derivative weight percent of oxidized CNFs and (3) overlay scan of various types of carbon nanofibers. OX = oxidized, AMM = ammonia treated, HHT = high heat treated, LHT = light heat treated, PS = pyrrolytically stripped (all fibers provided by Applied Sciences, Inc.).

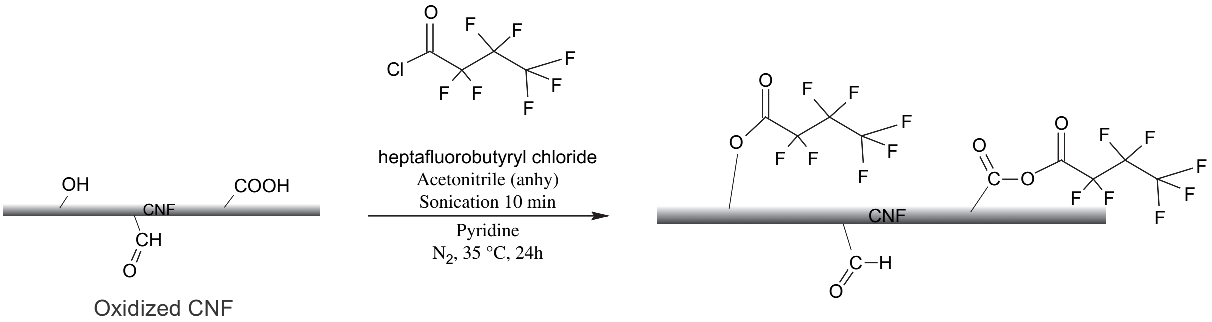

Scheme 2. Heptafluorobutyryl chloride reaction with oxidized CNFs and CNF-polyol.

which was decomposed with methanol. It is evident that there are still some residual hydroxyl groups (3400 cm^{-1}) present, although the relative height of the aliphatic CH_2 stretch (2950 cm^{-1}) and other peaks (1700–800 cm^{-1}) have increased considerably compared with the hydroxyl group peak. Despite all attempts, some water remained associated with the fibers. Hence, many of the hydroxyl groups were converted but the reaction was not quantitative.

From the resulting CNF-polyol *vs.* polyol CNF-F spectra it is evident that there is a decrease in the hydroxyl stretch at 3400 cm^{-1} relative to the aliphatic CH_2 at 2900 cm^{-1}. Since the polyol-based materials are not soluble in acetonitrile, the number of hydroxyl groups available to react with the acid chloride is reduced as compared to CNF-OX.

An estimation of the reactive oxygen group content was done using elemental analysis for fluorine of the fluorinated CNF samples. For the CNF-OX, assuming that all of the reactive oxygen groups are alcohols, by calculation, 5.1×10^{-5} moles of OH per gram or 3.1×10^{19} OH groups per gram are present. The amount of OH on the CNF-polyol was estimated to be 2.8×10^{-4} moles of OH per gram or 1.7×10^{20} OH groups per gram. This is an increase of 550% between the CNF-OX and the CNF-polyol. By theoretical calculation, if all reactive groups were alcohols and they all reacted with the fluorinated acid chloride, 12,800 ppm and 73,200 ppm F would have been obtained for the CNF-OX and CNF-polyol, respectively.

There are several reasons why this reaction was not quantitative; the major reason is aggregation of the oxidized groups in the acetonitrile. Acetonitrile was chosen for its low boiling point (close to the acid chloride). The CNF-OX is likely not fully dispersible and still aggregate in spite of the sonication. This prevents the reaction of some oxidized groups on the CNFs with the acid chloride, resulting in less than quantitative yield. There, fluorinated acid chloride also may not be completely soluble in acetonitrile.

In the aggregation study, *o*-DCB and water were chosen due to the solubility of polyol in water and the CNF-OX affinity for *o*-DCB. *o*-DCB is less polar and could not stabilize the hydrophilic polymer, and hence, the CNF-polyol collapsed into aggregates. If polymer was randomly attached, the areas of the CNF surface with polymer would be aggregated and areas of CNF without polymer would emanate outward into the *o*-DCB. In addition, the CNF-polyol showed complete aggregation in *o*-DCB, indicating that the polyol surface coating on CNFs caused complete aggregation. CNF-OX is more stable in the *o*-DCB than in water and the aggregation of CNF-OX in water was significantly more than in *o*-DCB, but less aggregated compared with CNF-polyol in *o*-DCB. The lack of significant aggregation was due to the CNFs having oxidized groups which partially stabilize the CNFs in water.

In the dispersion study, the CNF-polyol fibers remained suspended over time, while the CNF-OX settled out of solution. This is a good indication that there is a polymer coating on the surface of the CNF-polyol. The CNF-OX has 14 at% oxygen (determined by XPS), but the level of hydrophilicity was not enough to keep the fibers in solution indefinitely.

5. Conclusions

A hyperbranched polymer was grown in one-step from the surface of oxidized carbon nanofibers *via* a cationic polymerization of glycidol with boron trifluoride diethyl etherate. The hydroxyl content was determined through a reaction with a fluorinated acid chloride and it was found that the hydroxyl concentration increased by 550% for the glycidol-modified CNFs. These polymeric functionalized CNFs can be used to aid dispersion of CNFs in hydrophilic polymers or hydrophilic solvents.

Acknowledgements

Applied Sciences, Inc. for the carbon nanofiber samples, Case Western Reserve University for XPS measurements, Galbraith Laboratories for Elemental Analysis, and the Collaborative Center in Polymer Photonics (AFOSR, WPAFB) and the DURINT on Microstructure, Processing and Mechanical Performance of Polymer Nanocomposites, Air Force Contract No. F49620-01-1-0447 are gratefully acknowledged.

References

[1] Breuer O, Sundararaj U. Polym Compos 2004;25:630.
[2] Liu I, Huang H, Chang C, Tsai H, Hsu C, Tsiang R. Macromolecules 2004;37:283.
[3] Katz E, Willner I. Chem Phys Chem 2004;5:1084.

[4] Shim M, Kam N, Chen R, Li Y, Dai H. Nano Lett 2002;2:285.
[5] Wang J. Electroanalysis 2005;17:7.
[6] Lin Y, Taylor S, Li H, Fernando S, Qu L, Wang W, et al. J Mater Chem 2004;14:527.
[7] Bianco A, Prato M. Adv Mater 2003;15:1765.
[8] Webster T, Waid M, McKenzie J, Price R, Ejiofor J. Nanotechnology 2004;15:48.
[9] Lee C, Baker S, Marcus M, Yang W, Eriksson M, Hamers R. Nano Lett 2004;4:1713.
[10] Davis J, Coleman K, Azamian B, Bagshaw C, Green M. Chem Eur J 2003;9:3732.
[11] Tamanathan T, Fister F, Ruoff R, Brinson L. Chem Mater 2005;17:1290.
[12] Ramasubramanniam R, Chem J. Appl Phys Lett 2003;83:2928.
[13] Grujicic M, Cao G, Roy W. J Mater Sci 2004;39:4441.
[14] Lozano K, Bonilla-Rios J, Barrera E. J Appl Polym Sci 2001;80:1162.
[15] Kim H, Kim Y, Cho J, Hong J. Prog Org Coat 2003;48:34.
[16] Andrews R, Weisenberger M. Curr Opin Solid State Mater Sci 2004;8:31.
[17] Vander Wal RL, Ticich TM. J Phys Chem B 2001;105:10249.
[18] Ros T, Van Dillen A, Geus J, Koningsberger D. Chem Eur J 2002;8:1151.
[19] Sunder A, Hanselmann R, Frey H, Mulhaupt R. Macromolecules 1999;32:4240.
[20] Xinling W, Jianjun C, Ling H, Xiaozhen T. J Poly Sci B 2001;39:2225.
[21] Tokar R, Kubisa P, Penczek S, Dworak A. Macromolecules 1994;27:320.
[22] Royappa A, Vogt M, Sharma V. J Appl Polym Sci 2004;91:1344.
[23] Xu Y, Gao C, Kong H, Yan D, Jin Y, Watts P. Macromolecules 2004;37:8846.
[24] Hong C, You Y, Wu D, Liu Y, Pan C. Macromolecules 2005;38:2606.
[25] Hu H, Bhowmik P, Zhao B, Hamon MA, Itkis ME, Haddon RC. Chem Phys Lett 2001;345:25.
[26] Huang W, Kim J, Bruening M, Baker G. Macromolecules 2002;35:1175.
[27] Lakshminarayanan PV, Toghiani H, Pittman Jr CU. Carbon 2004;42:2433.